An evaluation of computed tomography dose index measurements using a pencil ionisation chamber and small detectors

Choirul Anam[1,5] , **Toshioh Fujibuchi[2], Freddy Haryanto[3], Rena Widita[3], Idam Arif[3] and Geoff Dougherty[4]**

[1] Department of Physics, Faculty of Mathematics and Natural Sciences, Diponegoro University, Jl. Prof. Soedarto SH, Tembalang, Semarang 50275, Central Java, Indonesia

[2] Department of Health Sciences, Faculty of Medical Sciences, Kyushu University, 3-1-1 Maidashi, Higashi-ku, Fukuoka, Fukuoka 812-8582, Japan

[3] Department of Physics, Faculty of Mathematics and Natural Sciences, Bandung Institute of Technology, Ganesha 10, Bandung 40132, West Java, Indonesia

[4] Department of Applied Physics and Medical Imaging, California State University Channel Islands, Camarillo, CA 93012, United States of America

E-mail: anam@fisika.undip.ac.id

Abstract

The aim of this study was to compare the values of the computed tomography dose index 100 ($CTDI_{100}$) obtained using two small detectors (i.e. a small ionisation chamber and a small solid state detector) with those obtained from a 100 mm pencil ionisation chamber for various input CT parameters: beam width, kVp, mAs, pitch, and head-body phantom variation. The measurement of $CTDI_{100}$ using the 100 mm pencil chamber was carried out in a single rotation of axial mode, while the measurement using small detectors was carried out in helical mode. The differences of $CTDI_{100}$ values obtained with two small detectors were about 7% for all variations. The differences of $CTDI_{100}$ values obtained with small detectors and a 100 mm pencil ionisation chamber for beam widths of more than 4 mm were within 40%. However, for the narrowest beam widths (4 mm), the difference between them was very large (about 150%).

Keywords: CT dosimetry, computed tomography dose index, small detector, small ionisation chamber, pencil ionisation chamber, CT dose profiler

(Some figures may appear in colour only in the online journal)

[5] Author to whom any correspondence should be addressed.

1. Introduction

A 100 mm pencil ionisation chamber [1] and a cylindrical polymethyl methacrylate (PMMA) phantom of approximately 150 mm length has been the standard for measuring the dose index of CT scanners [2, 3], and the computed tomography dose index 100 ($CTDI_{100}$) is obtained from this measurement [4, 5]. This metric is used to characterise the radiation output of CT scanners, but is not meant to estimate individual patient dose [6]. A metric for estimating individual patient dose is the size-specific dose estimate (SSDE) [7]. The SSDE is calculated based on the concepts of CTDI, so that an accurate CTDI estimate lead to an accurate estimate of patient dose [8, 9].

There was no debate about the efficacy of the 100 mm pencil ionisation chamber and the resulting $CTDI_{100}$ value [10–13] until the introduction of multi-detector CT (MDCT) technology [14, 15], which enabled scanning using beam widths up to 40 mm or more [16]. It is clear that a large amount of radiation scattering outside the length of 100 mm is not measured by the 100 mm pencil chamber [15, 17]. Moreover, after the introduction of the cone-beam CT (CBCT), which enabled a scan coverage of 100 mm in one scan rotation [18], more scatter radiation is missed by the 100 mm pencil chamber.

Studies had been carried out using combinations of several PMMA phantoms up to 900 mm long [15–18] in order to evaluate the concept of $CTDI_{100}$. In these studies, an equilibrium dose was introduced, which is the maximal dose of total primary radiation and scattering radiation whose value does not increase with additional integration length along the z-axis [19, 20]. This equilibrium dose occurs at an integration length of about 450 mm. These studies showed that the efficiency of the $CTDI_{100}$ values (i.e. $CTDI_{100}$ / $CTDI_{\infty}$) [19] were only about 73% and 56% at the center of the head and body PMMA phantoms, and about 85% and 82% at the periphery of head and body PMMA phantoms, respectively [15].

In these evaluations of the efficiency and accuracy of $CTDI_{100}$, the 100 mm pencil chamber cannot be used [19, 20]. The evaluations were performed by using small ionisation chambers [18], and using other types of detectors such as optically stimulated luminescence (OSL) detectors [15], pin photodiode sensors [16] and lithium fluoride (LiF) TLDs [21]. Evaluations were also performed using Monte Carlo simulation [17, 22, 23]. All these studies showed the limit of accuracy, practical utility and clinical relevance for $CTDI_{100}$, which excludes the contributions of radiation scattered beyond the 100 mm range of integration along z-axis. In addition, previous study showed that the underestimation of $CTDI_{100}$ is systematic, applying to both narrow and wide beams, and is greater for increasing z-axis collimation [22].

Dixon recommended the use of moving a small ionisation chamber in helical mode to obtain dose profiles and CT dose index values [19]. The advantages are that the small chamber can be moved to obtain a dose profile with a specific length to reach the dose equilibrium, and the ease of calibration. This concept was adopted by AAPM TG 111 [24], in which it was stated that if the profile dose obtained by the small ionisation chamber is integrated along the 100 mm to obtain $CTDI_{100}$ then the result would be comparable with that obtained using a 100 mm pencil ionisation chamber [24]. However, to the best of our knowledge, no studies have been performed to compare actual $CTDI_{100}$ values obtained using a small ionisation chamber against the 100 mm pencil chamber for various input parameters.

This study aims to compare the value of $CTDI_{100}$ obtained with a small ionisation chamber with a 100 mm pencil ionisation chamber for various input CT parameters. We also compare the results with those obtained using a small solid state detector, known as a CT dose profiler [25].
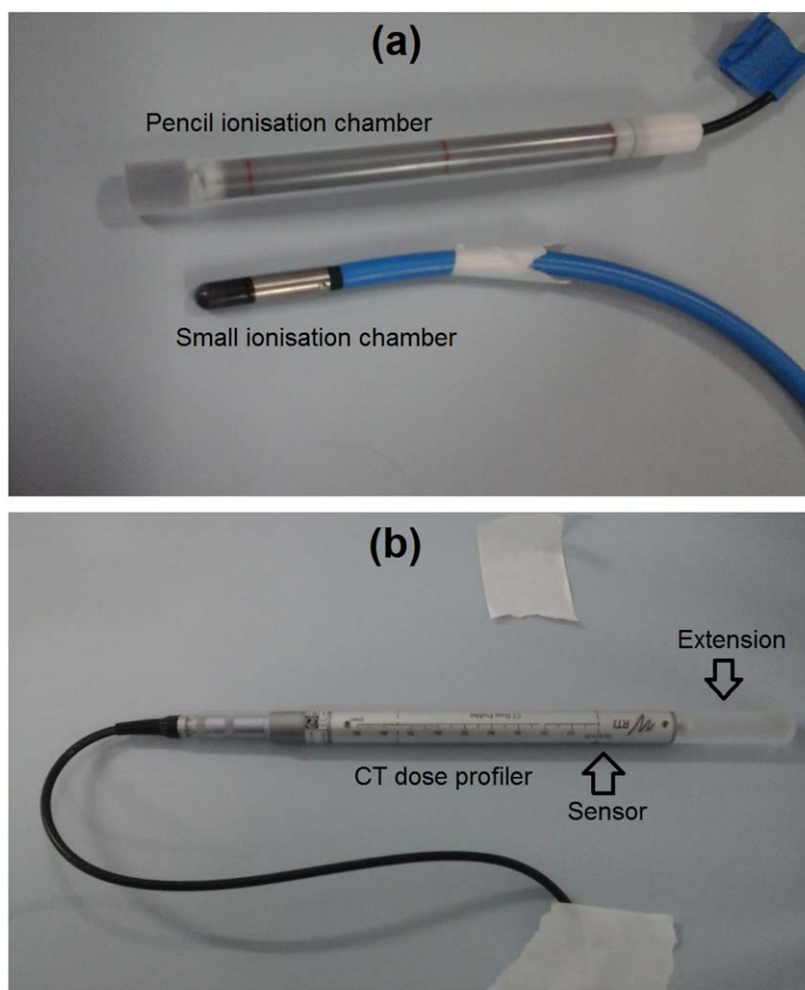
Figure 1. Three types of detectors used in $CTDI_{100}$ measurements, namely (a) small ionisation chamber and pencil ionisation chamber and (b) small solid state detector.

2. Methods

2.1. Detectors

In this study two small moving detectors, namely a small ionisation chamber (figure 1(a) below) and a small solid detector (figure 1(b)), were used to measure dose profiles and $CTDI_{100}$. The $CTDI_{100}$ results were then compared with the results from a pencil ionisation chamber (figure 1(a) above).

The pencil ionisation chamber used in this study was a Radcal 10×6-3CT with a length of 100 mm, connected to a Radcal Accu-Dose (S2186-SS) electrometer. This dosimeter was calibrated at JQA (Japan Quality Assurance Organisation). The uncertainty of this dosimeter was $\pm 6\%$ with a confidence interval of 68%. The small ionisation chamber had a volume of 0.125 cc (PTW N31005 ion chamber serial number: 0543 (Freiburg, Germany)). The PTW N31005 was calibrated in air with 120 kV x-rays using a 6 cm^3 ionisation chamber dosimeter

(10 × 6-6, Radcal) at Kyushu University, and proofread by JQA (Japan Quality Assurance Organisation). The uncertainty of this dosimeter was ±10% with a confidence interval of 68%. It was connected to an electrometer (EMF521 (EMF Japan Co. Ltd, Japan)) and data transferred to a netbook using EMF521 software (EMF Japan Co. Ltd, Japan). The sampling rate of dose measurement was two samples/s. The dose data was collected in units of nC and automatically converted to mGy units.

The width of the small solid-state detector was 0.25 mm. The detector was integrated into a probe called a CT dose profiler (RTI Electronic, Sweden). The probe had a shape like the pencil ionisation chamber with a diameter of 12.5 mm and length of 165 mm. This dosimeter used the calibration value indicated by the manufacturer at the time of purchase. The uncertainty of this dosimeter was ±3% with a confidence interval of 68%. The dosimeter can be inserted into the holes of the PMMA phantom. The probe had an extension piece made of 45 mm PMMA, so the detector could be centered in the middle of a 150 mm PMMA phantom when the end of the extension reached the end of the phantom. The CT dose profiler was then coupled to a Barracuda electrometer (RTI Electronic, Sweden), whose output was connected to a netbook running Ocean software. The CT dose profiler recorded the dose at high sampling rates (up to 2000 samples/s), in units of mGy.

2.2. Mode of measurements

The $CTDI_{100}$ measurements using the 100 mm pencil ionisation chamber pencil were taken in axial mode [3, 4]. The pencil chamber was positioned in the center of the PMMA phantom and the scanning carried out in the middle of the phantom position. The measurement of CT dose using the pencil ionisation chamber gave the accumulative dose along 100 mm directly (dose profile integral along 100 mm, DPI_{100}).

$$DPI_{100} = \int_{z=-50\,mm}^{+50\,mm} D(z)dz. \tag{1}$$

Dividing DPI_{100} by the nominal beam width (NT) gives the value of the CT dose index 100 ($CTDI_{100}$):

$$CTDI_{100} = \frac{DPI_{100}}{NT}. \tag{2}$$

In helical mode, there is an additional factor called pitch factor [26]. The pitch factor is the speed of the patient table translation per gantry rotation. With helical mode there is an overlapping of the scanning area for pitches smaller than 1, and a scanning gap for pitches above 1. The pitch factor is formulated as:

$$P = \frac{\Delta d}{NT}, \tag{3}$$

where Δd is the distance of table translation per single tube rotation of 360°, N is the number of detectors and T is the width of the detector. In helical mode, the $CTDI_{100}$ value is corrected by pitch factor, so that $CTDI_{vol}$ is obtained [26]:

$$CTDI_{vol,100} = \frac{CTDI_{100}}{P}. \tag{4}$$

A major limitation of dose measurements using a 100 mm pencil ionisation chamber is that they can only measure doses of 100 mm length. However, using small detectors allow the scanning length to be longer than 100 mm. Our measurements with these small detectors used helical mode [24] as shown in figure 2. As illustrated in figure 2(a) when the scan is still on
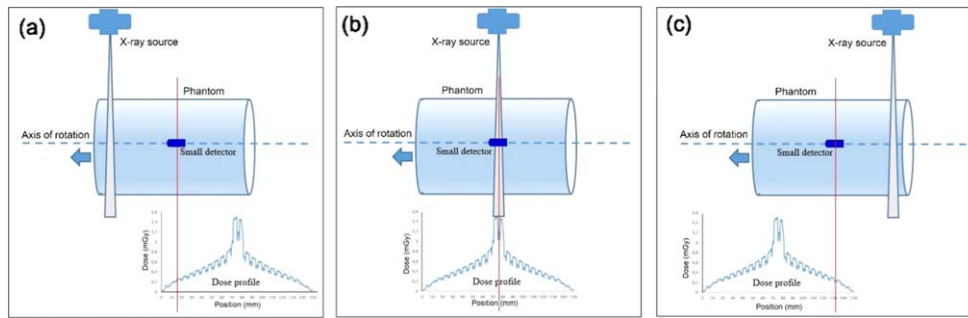
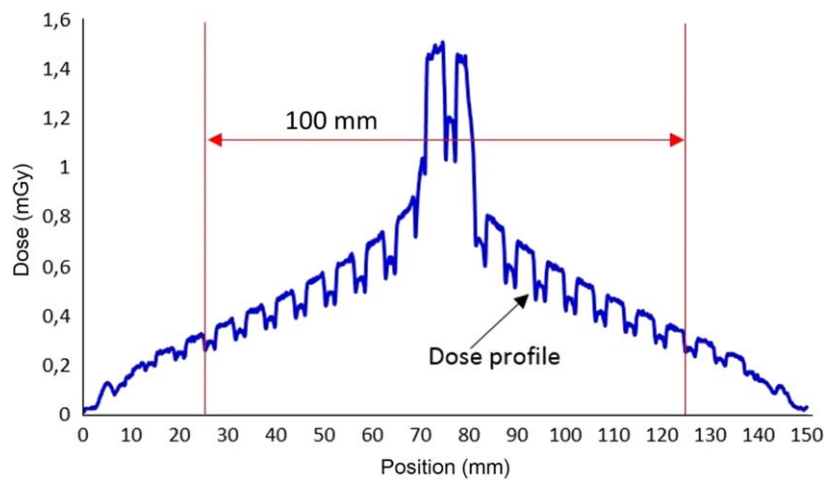**Figure 2.** Illustration of measurements of dose profile using small moving detector in helical mode.

Figure 3. Example of profile dose along 150 mm. If the dose profile is integrated along 100 mm, then DPI_{100} will be obtained. Dividing DPI_{100} by the nominal beam width, $CTDI_{100}$ is obtained.

the left end of the phantom, the small detector (placed in the middle of the phantom) measures only the scattering radiation from the left side of phantom. As the scan progresses, the small detector moves steadily along with the phantom and the patient table movement, and detects a larger scattering dose. When the small detector is at the position shown in figure 2(b), the radiation beam scans the middle of the phantom and the small detector measures the primary dose. Next, as the small detector moves to the left as shown in figure 2(c), it measures only the scattering radiation from the scanning area at the right end of the phantom.

The data collected by the small detector is sent to the electrometer and netbook, and a profile dose of a certain length is obtained (figure 3). By integrating this dose profile the value of DPI is obtained:

$$DPI = \int D(z)dz. \tag{5}$$

If the integration is carried out for a length of 100 mm, then a DPI_{100} value will be obtained which should be comparable to that obtained using 100 mm pencil ionisation chamber.

$$DPI_{100} = \int_{-50\,mm}^{50\,mm} D(z)dz. \tag{6}$$

In contrast to the pencil ionisation chamber which must include the pitch value for dose estimation in helical mode, the dose measurement using the small moving detector has inherently incorporated the pitch value in the measurement, so there is no need for any pitch correction. With a small moving detector, the effect of pitch is directly visible on the dose profile.

2.3. Input parameters

In this study, $CTDI_{100}$ measurements were acquired on a Toshiba Alexion 4-slice CT scanner installed in Kyushu University, Japan. The $CTDI_{100}$ comparisons were evaluated at a variety of input CT parameters: variations of beam width, kVp, mAs, pitch, and head-body phantom variation. Variations of beam width were 4, 8, 12 and 16 mm, with other parameters kept constant (100 mA, 120 kVp, pitch of 0.875, and 1 s rotation time). Variations of tube voltages were 80, 100, 120 and 135 kVp with other parameters kept constant (100 mA, pitch of 0.875, 8 mm beam width, and 1 s rotation time), variations of tube currents were 25, 50, 100, 120 and 140 mA with other parameters kept constant (120 kVp, pitch of 0.875, 8 mm beam width and 1 s rotation time), variations of pitches were 0.75, 0.875, 1.375 and 1.5 with other parameters kept constant (100 mA, 120 kVp, 8 mm beam width and 1 s rotation time). Measurements were performed on the body and head PMMA phantoms (measured at beam width 8 mm, 120 kVp, 100 mA, pitch of 0.875 and 1 s rotation time).

3. Results

3.1. Dose profiles

The profiles of doses for several different variables measured using the small solid state detector and the small ionisation chamber are shown in figure 4. Beam width variations ranging from 4 mm to 16 mm measured using the small solid state detector are shown in figure 5(a), and using the small ionisation chamber in figure 4(b). Tube voltage variations ranging from 80 kVp to 135 kVp measured using a small solid state detector are shown in figure 4(c), and using the small ionisation chamber in figure 4(d). Tube current variations ranging from 25 mA to 120 mA measured using a small solid state detector are shown in figure 4(e), and using the small ionisation chamber in figure 4(f). Pitch variations ranging from 0.75 to 1.5 measured using a small solid state detector are shown in figure 4(g), and using the small ionisation chamber in figure 4(h). The variation of head-body PMMA phantom as measured using small solid state detector are shown in figure 4(i), and using the small ionisation chamber in figure 4(j).

Figure 4 shows that profiles measured using a small ionisation chamber are comparable to that obtained using a small solid state detector for all input parameter variations. However, profiles obtained using a small solid state detector are more jagged (fluctuating) than those obtained using a small ionisation chamber. This is because of the larger sampling rate of the small solid detector (viz. 62 samples/s), compared with the sampling rate of the small ionisation chamber (viz. 2 samples/s).
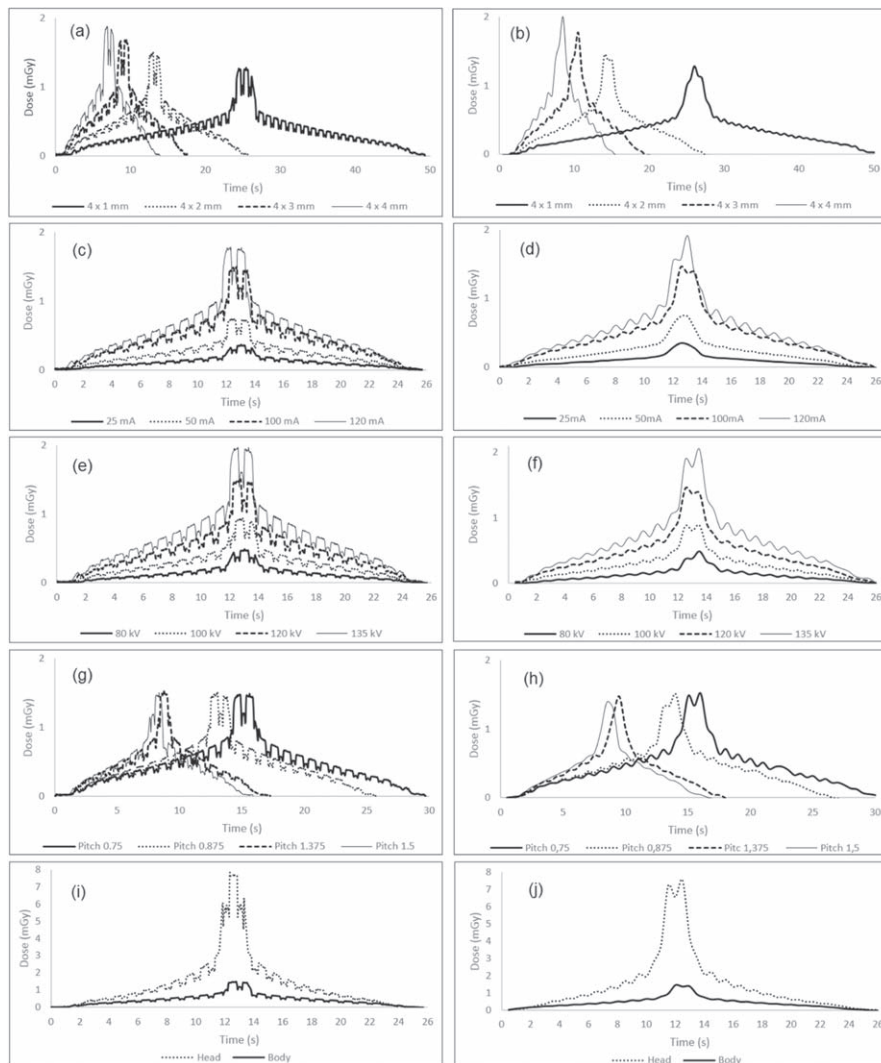
Figure 4. Dose profiles measured using a small solid state detector (left) and a small ionisation chamber (right) with different beam parameters (a), (b) variations of beam width, (c), (d) tube current variation, (e), (f) tube voltage variation, (g), (h) different pitches and (i), (j) head-body phantoms. Dose profiles for the tube current, tube voltage, pitch and head body variations were measured at bean width of 2×4 mm.

3.2. DPI values

If the *X*-axis of figure 4 is converted to a distance and the profile is integrated, an integral dose profile (DPI) will be obtained (table 1). The DPI_{100} values obtained using a small ionisation chamber are slightly larger (by <10%) than those obtained using a small solid state detector. It shows that the wider beam width and pitch values (all other input parameters being kept constant) result in smaller DPI_{100} values, due to the rapidly increasing phantom translation and small detector movement. Conversely, a rise in tube voltage and current causes the
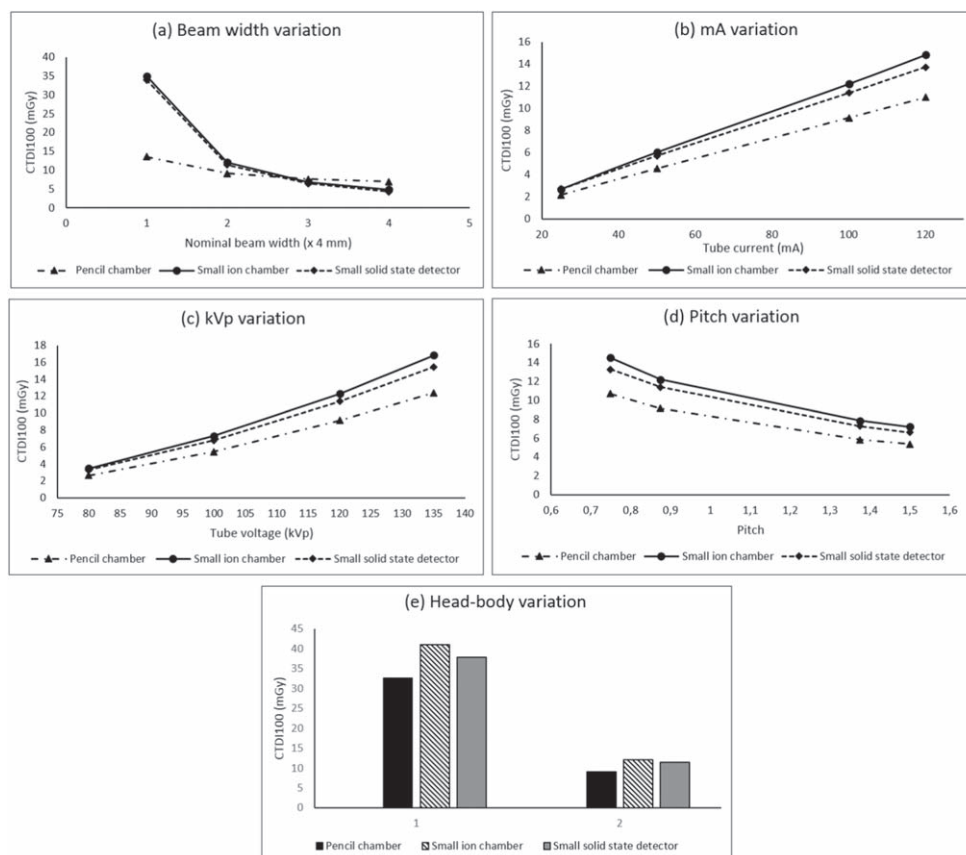
Figure 5. CTDI$_{100}$ values measured using 100 mm pencil ionisation chamber, small ionisation chamber and small solid state for variations of (a) beam width, (b) tube current variation, (c) tube voltage variation, (d) pitch variation and (e) head-body phantom variation. CTDI$_{100}$ values for the tube current, tube voltage, pitch and head body variations were measured at a beam width of 2×4 mm.

increasing DPI$_{100}$ value. The DPI$_{100}$ value inside the head phantom is greater than in body phantom by $>300\%$.

3.3. CTDI$_{100}$ values

Various CTDI$_{100}$ values measured using a small ionisation chamber, a small solid state detector and also using a 100 mm pencil ionisation chamber are shown in figure 5. The CTDI$_{100}$ values obtained using the small ionisation chamber and the small solid state detector are very similar for all variations. The differences between CTDI$_{100}$ values obtained with small ionisation chamber and small solid state detector are listed in table 2. It is shown that CTDI$_{100}$ differences are about 7%.

The differences between CTDI$_{100}$ values obtained with small moving detectors and a 100 mm pencil ionisation chamber for beam width 8–16 mm are within 40%. However, for the narrowest beam width (4 mm), the differences between small detectors and the 100 mm pencil ionisation chamber are about 150%.

Table 1. DPI_{100} values measured using a small ionisation chamber and, alternatively, a small solid state detector.

Variations	DPI_{100} using a small ionisation chamber (mGy-mm)	DPI_{100} using a small solid state detector (mGy-mm)	DPI_{100} using a pencil ionisation chamber (mGy-mm)[a]
Beam width (mm)			
1×4	140.1	135.9	54.4
2×4	97.8	91.3	73.4
3×4	82.8	77.6	92.1
4×4	78.6	68.1	111.8
Tube current (mA)			
25	21.8	22	17.6
50	48.4	46	36.6
100	97.8	91.3	73.4
120	118.8	109.8	88.1
Tube voltage (kVp)			
80	28.1	26.3	21.5
100	58.7	54.5	43.8
120	97.8	91.3	73.4
135	134.7	123.8	99.2
Pitch			
0.75	116.3	106.3	85.6
0.875	97.8	91.3	73.4
1.375	62.8	58.3	46.7
1.5	57.7	53	42.8
Phantom (body-head)			
Body	97.8	91.3	73.4
Head	327.7	302.2	260.8

[a] After it was corrected for pitch.

4. Discussion

Profiles doses for all variations appear to be jagged (figure 4), due to the influence of the patient table [25]. When the source of the x-ray beam is above the phantom, x-rays directly impinged the phantom, but when the x-ray beam source is below the phantom the x-rays are absorbed by the patient table prior to the phantom. As a result, when an x-ray source is above the phantom, the measured dose of a small detector is greater than that when the x-ray source is below the phantom.

The $CTDI_{100}$ values obtained using the small detectors (i.e. small ionisation chamber and the small solid state detector) are very comparable for all variations with differences of about 7%. These differences are within the uncertainties of these detectors ($\pm 10\%$ for small ionisation chamber and $\pm 3\%$ for solid state detector). The $CTDI_{100}$ values obtained with small detectors and a 100 mm pencil ionisation chamber are interesting. The difference in $CTDI_{100}$ values measured using a pencil chamber and a small detector is strongly influenced by beam width. With a 4 mm beam width, the difference is about 150%, and the difference

Table 2. Differences between $CTDI_{100}$ values measured using the three detectors, namely a small ionisation chamber, a small solid state detector and a 100 mm pencil ionisation chamber.

Variations	Δ pencil-small ion chamber (%)	Δ pencil-small solid state (%)	Δ small ion-small solid state (%)
Beam with (mm)			
1 × 4	157.5	149.8	3
2 × 4	33.4	24.4	6.7
3 × 4	−10.1	−15.9	6.4
4 × 4	−29.7	−39.2	13.4
Tube current (mA)			
25	23.5	24.9	−1.1
50	32.2	25.7	5
100	33.4	24.4	6.7
120	34.9	24.9	7.5
Tube voltage (kVp)			
80	30.9	22.7	6.3
100	34	24.3	7.2
120	33.4	24.4	6.7
135	35.8	24.9	8.1
Pitch			
0.75	35.9	24.2	8.6
0.875	33.4	24.4	6.7
1.375	34.5	24.9	7.1
1.5	34.8	24.3	8.2
Phantom (body-head)			
Body	25.7	15.9	7.8
Head	33.4	24.4	6.7

decreases with the increase of beam width. With a 8 mm beam width, the difference is within 40%, and with a 12 mm beam width, the difference is within 10%. After varying the beam width, we then varied the scan parameters (kVp, mA, pitch, and phantom) with a beam width 8 mm. The results were consistent for all variations, i.e. with a difference between 23%–36%. These differences, especially in the 4 mm beam width, convincingly show the different nature of the pencil chamber and small detectors, because the differences are much greater than the uncertainty of each dosimeter, i.e. within ±10%.

These results agree with the comments in AAPM TG 111 that the $CTDI_{100}$ values obtained using a 100 mm pencil chamber and a small detector are comparable [24], except for the narrowest beam width (4 mm). With our experimental results, we have been able to verify that $CTDI_{100}$ calculations (for beam widths more than 4 mm) can be performed with acceptable accuracy using small detectors. The use of these small detectors have the advantage of being able to measure the dose for any desired z-length, facilitating the measurement of equilibrium doses [20].

However, the difference between small detectors and the 100 mm pencil ionisation chamber is very significant for beam widths of 4 mm. This is likely due to collimation inaccuracy at the smallest beam widths. The beam width measured using a small solid state detector in the air were 8.1, 11.7, 14.5 and 20.4 mm for beam width settings of 4, 8, 12 and 16 mm, respectively. The percentage difference was about 100% for the smallest beam width (4 mm), but the percentage difference was smaller for wider beam widths. The results are

consistent with a previous study by Jackson *et al* [27]. The beam width inaccuracy using a small detector is higher than with a pencil chamber due to the nature of helical scanning. In helical scanning, beam width inaccuracy occurs over many rotations during the scanning process, while in axial scanning it occurs only in a single rotation. This is why the $CTDI_{100}$ for narrow beam widths measured using small detectors is greater than that when using a 100 mm pencil chamber.

In view of this, we argue that the $CTDI_{100}$ values obtained using small moving detectors illustrate the true nature of the output dose of a CT scan over scan coverage areas with multiple scanning (for both axial and helical modes). $CTDI_{100}$ values measured using a 100 mm pencil ionisation chamber only include over-beaming from a single scan, while the patient gets multiple scans. Therefore, measurements using a small moving detector for very narrow beam widths can be considered more realistic in depicting the nature of the output dose than using a 100 mm pencil ionisation chamber.

Based on this finding, the accuracy of the estimate CT output ($CTDI_{100}$) using a 100 mm pencil chamber should be considered carefully not only for wide beam widths (more than 40 mm), as has been reported elsewhere [15–17, 19–22], but also for very narrow beam widths. An accurate $CTDI_{100}$ measurement is very important for an estimate of individual patient's dose in terms of size-specific dose estimate [28, 29].

Our study was limited in that measurements were only performed on one type of CT scanner and only in the central hole of the phantom. Further evaluation of this phenomenon will be performed on other CT scanners and in the phantom peripheral axis.

5. Conclusions

$CTDI_{100}$ calculations using two small detectors (a small ionisation chamber and a small solid state detector) and 100 mm pencil ionisation chamber as standard tools are comparable for all variations of CT input parameters except for the narrowest beam widths (~4 mm). CTDI measurements using small detectors have better flexibility compared to 100 mm pencil ionisation chamber, because small moving detectors can be used to measure the dose profile for any desired length, allowing for the measurement of more scatter doses of wide beam widths from MDCT and CBCT technology.

ORCID iDs

Choirul Anam https://orcid.org/0000-0003-0156-6797

References

[1] Suzuki A and Suzuki M N 1978 Use of a pencil shaped ionization chamber for measurement of exposure resulting from a computed tomography scan *Med. Phys.* **5** 536–9

[2] American Association of Physicists in Medicine 2008 AAPM report no. 96. The measurement, reporting and management of radiation dose in CT (www.aapm.org/pubs/reports/RPT_96.pdf) (Accessed: 31 January 2014)

[3] McNitt-Gray M F 2002 AAPM/RSNA physics tutorial for residents: topics in CT–radiation dose in CT *RadioGraphics* **22** 1541–53

[4] Kalender W A 2014 Dose in x-ray computed tomography *Phys. Med. Biol.* **59** R129–50

[5] Goldman L W 2007 Principles of CT: radiation dose and image quality *J. Nucl. Med. Technol.* **35** 213–25

[6] McCollough C H, Leng S, Lifeng Y, Cody D D, Boone J M and McNitt-Gray M F 2011 CT dose index and patient dose: they are not the same thing *Radiology* **259** 311–6

[7] American Association of Physicists in Medicine 2011 Size-specific dose estimates (SSDE) in pediatric and adult body CT examinations (report no. 204) (College Park, MD: American Association of Physicists in Medicine) (www.aapm.org/pubs/reports/rpt_204.pdf) (Accessed: 4 February 2015)

[8] Anam C, Haryanto F, Widita R, Arif I and Dougherty G 2016 Automated calculation of water-equivalent diameter (D_W) based on AAPM task group 220 *J. Appl. Clin. Med. Phys.* **17** 320–33

[9] Anam C, Haryanto F, Widita R, Arif I, Dougherty G and McLean D 2017 The impact of patient table on size-specific dose estimate (SSDE) *Australas. Phys. Eng. Sci. Med.* **40** 153–8

[10] American Association of Physicists in Medicine 1993 AAPM report no. 39. Specification and acceptance testing of computed tomography scanners (https://aapm.org/pubs/reports/rpt_39.pdf) (Accessed: 2 March 2009)

[11] International Atomic Energy Agency 2012 IAEA human health series no. 19. Quality assurance programme for computed tomography: diagnostic and therapy applications (https://pub.iaea.org/MTCD/Publications/PDF/Pub1557_web.pdf) (Accessed: 13 October 2013)

[12] Brenner D J, McCollough C H and Orton C G 2006 It is time to retire the computed tomography dose index (CTDI) for CT quality assurance and dose optimization *Med. Phys.* **33** 1189–91

[13] McCollough C H and Zink F E 1999 Performance evaluation of a multi-slice CT system *Med. Phys.* **26** 2223–30

[14] Prokop M 2005 New challenges in MDCT *Eur. Radiol. Suppl.* **15** E35–45

[15] Ruan C, Yukihara E G, Clouse W J, Gasparian P B R and Ahmad S 2010 Determination of multislice computed tomography dose index (CTDI) using optically stimulated luminescence technology *Med. Phys.* **37** 3560–8

[16] Mori S, Endo M, Nishizawa K, Tsunoo T, Aoyama T, Fujiwara H and Murase K 2005 Enlarged longitudinal dose profiles in cone-beam CT and the need for modified dosimetry *Med. Phys.* **32** 1061–9

[17] Li X, Zhang D and Liu B 2012 Estimation of the weighted CTDI for multislice CT examinations *Med. Phys.* **39** 901–5

[18] Kim S, Song H, Samei E, Yin F and Yoshizumi T T 2010 Computed tomography dose index and dose length product for cone-beam CT: Monte Carlo simulations of a commercial system *J. Appl. Clin. Med. Phys.* **12** 84–95

[19] Dixon R L 2003 A new look at CT dose measurement: beyond CTDI *Med. Phys.* **30** 1272–80

[20] Dixon R L and Ballard A C 2007 Experimental validation of a versatile system of CT dosimetry using a conventional ion chamber: beyond CTDI 100 *Med. Phys.* **34** 3399–413

[21] Nakonechny K D, Fallone B G and Rathee S 2005 Novel methods of measuring single scan dose profiles and cumulative dose in CT *Med. Phys.* **32** 98–109

[22] Boone J M 2007 The trouble with CTDI100 *Med. Phys.* **34** 1364–71

[23] Boone J M 2009 Dose spread functions in computed tomography: a Monte Carlo study *Med. Phys.* **36** 4547–54

[24] American Association of Physicists in Medicine 2010 AAPM report no. 111. The future of CT dosimetry: comprehensive methodology for the evaluation of radiation dose in x-ray computed tomography (https://aapm.org/pubs/reports/RPT_111.pdf) (Accessed: 15 December 2013)

[25] Anam C, Haryanto H, Widita R, Arif I and Dougherty G 2016 Profile of CT scan output dose in axial and helical modes using convolution *J. Phys.: Conf. Ser.* **694** 012034

[26] Wang G and Vannier M W 1999 The effect of pitch in multislice spiral/helical CT *Med. Phys.* **26** 2648–53

[27] Jackson S R, Ahmad S, Hu Y and Ruan C 2013 Evaluation of different techniques for CT radiation profile width measurement *J. Appl. Clin. Med. Phys.* **14** 227–37

[28] Anam C, Haryanto F, Widita R, Arif I and Dougherty G 2017 The size-specific dose estimate (SSDE) for truncated computed tomography images *Radiat. Prot. Dosim.* **175** 313–20

[29] Anam C, Fujibuchi T, Toyoda T, Sato N, Haryanto F, Widita R, Arif I and Dougherty G 2018 A simple method for calibrating pixel values of the CT localizer radiograph for calculating water-equivalent diameter and size-specific dose estimate *Radiat. Prot. Dosim.* **179** 158–68